JOURNAL OF CATALYSIS 121, 99–109 (1990)

Surface Composition and Reactivity of Lithium-Doped Magnesium Oxide Catalysts for Oxidative Coupling of Methane

X. D. PENG, D. A. RICHARDS, AND P. C. STAIR

Department of Chemistry, Northwestern University, Evanston, Illinois 60208

Received May 2, 1989; revised August 8, 1989

Lithium-doped magnesium oxide catalysts for oxidative coupling of methane with lithium loadings ranging from 0.02 to 10 wt% have been studied using both kinetic and XPS measurements. A correlation between CH_4 conversion and the concentration of surface species corresponding to an O(1*s*) XPS peak at 533.0 eV has been obtained. These active species were assigned to Li^+O^- centers formed by substituting Li into MgO lattices. © 1990 Academic Press, Inc.

INTRODUCTION

In 1982, Keller and Bhasin (*1*) first reported the screening of metal oxides as catalysts for oxidative coupling of methane into ethane and ethylene using dioxygen as the oxidant. This initial study demonstrated that a large number of metal oxides were active for this reaction. Highest ethane and ethylene selectivity was obtained from the catalysts capable of cycling between at least two oxidation states (Sn, Pb, Sb, Bi, Tl, Cd, and Mn). Since then, considerable attention has been given to developing and improving catalysts for methane oxidative coupling (*2–20*). Among the variables having been studied are support (*2, 3*), surface acidity (*4*), promotor (*5–7*), and a survey of other oxides (*8–14*). There is a general consensus that methane activation takes place primarily due to H atom abstraction at the catalyst surface, forming gas-phase methyl radicals. The detailed mechanism of methane coupling, however, has been clouded by secondary reactions of the methyl radical which may take place both on catalyst surfaces and in the gas phase. A review of this subject has been given recently by Lee and Oyama (*15*).

Lithium-doped magnesium oxide catalysts, first reported by Lunsford *et al.* (*16, 17*), represent a special category among all the metal oxide catalysts examined. Unlike the system reported by Keller and Bhasin (*1*), the metal components in this catalyst are irreducible. Also, as noted by Lee and Oyama (*15*), this catalyst appears to be the only one in which the methane activation sites have been identified, i.e., Li^+O^- centers formed by substituting Li into MgO lattices. The identification of these active species is based on a correlation between the concentrations of the Li^+O^- center and gas-phase methyl radicals, both of which were monitored by EPR (*16, 17*). It has been proposed that the Li^+O^- site can abstract a proton from methane, yielding a methyl radical and a Li^+OH^- site. The latter is converted back to Li^+O^- through reaction with gas-phase oxygen. Similar results have been reported recently on Li/ZnO (*18*) and Na/CaO (*19*) catalysts by the same group, suggesting that, in general, the O^- site formed by the substitution of alkali for the divalent metal ion is responsible for methane activation.

Although alkali metal-related species have been proposed to be responsible for methane activation, the correlation between CH_4 conversion and alkali metal loading has not been observed in all the studies carried out over the Li/MgO type of catalysts (*6, 16–20*). In general, the CH_4 conversion levels off or becomes scattered

0021-9517/90 $3.00

at high loadings. In addition, the direct correlation between Li^+O^- concentration and CH_4 conversion has not been observed. For instance, in the study of Lunsford *et al.*, the maximum Li^+O^- concentration was observed from a catalyst with a 13.5 wt% lithium loading (*17*), while over catalysts with lithium loadings in the range 0.2 to 26 wt% the CH_4 conversion exhibited a maximum around 1.0 wt% lithium loading and a rather constant activity from 7 to 26 wt% (*16*). The lack of the correlation may result from either of the following reasons. First, the actual surface lithium concentration may differ from the original lithium loading due to migration into the bulk and/or the loss of lithium to the gas phase under reaction conditions. It has been reported that 40 ± 10% of Na^+ and 90 ± 10% of Rb^+ are lost during heat treatment at 800°C from the Na^+- and Rb^+-doped MgO catalysts (*10*). Secondly, the attempt to correlate CH_4 conversion with any solid-phase property may be hindered by the bulk sensitive nature of the EPR analytic technique used in the reported studies. In any case it is important to determine the surface composition of the catalysts under the reaction conditions. In the current investigation, XPS was used to monitor the surface composition of Li/MgO oxidative coupling catalysts with different lithium loadings, in conjunction with traditional kinetic measurements, in an effort to correlate surface properties with catalyst activity.

EXPERIMENTAL

Lithium-doped magnesium oxide catalysts were prepared in a method similar to that of Lunsford (*16*). Lithium precursors ($LiOH \cdot H_2O$, Aldrich, lot No. 02205EP) and MgO (Aldrich, lot No. 00931CT) were mixed together in deionized water. The resulting slurry was heated with stirring to evaporate excess water until a thick paste remained. The catalyst was then dried at 120°C in an oven for several hours prior to being ground into powders. Each sample was calcined in dioxygen at 460°C for 2 h just prior to starting the reaction.

Kinetic studies were performed in a flow system constructed of quartz and stainless-steel tubing. The reactor was a section of quartz tubing 2.5 cm o.d. and 36 cm long attached to a second section of quartz tubing 0.6 cm o.d. and 18 cm long. The catalyst was held just above the union of the two sections to limit the free space in the reactor beyond the catalyst bed, and thus reduce secondary gas-phase reactions. Since it was observed that (1) lithium could migrate easily onto the walls of the quartz reactor at reaction temperature (650°C), and (2) the lithium-doped quartz was active for methane conversion, the catalyst was held in a gold bucket to prevent lithium from migrating onto the walls of the quartz reactor. With this setting, the CH_4 conversion in the absence of catalysts was below 2% under the reaction conditions.

The oxygen used in this study was UHP further purified by passing over a bed of Pt/SiO_2 to remove hydrogen and a bed of molecular sieve to remove water. Methane (UHP) was used without further purification. Helium, used as a diluent, was UHP further purified by passing over a bed of MnO/SiO_2 to remove oxygen and a bed of molecular sieve to remove water. The standard reactant feed was 130 Torr methane, 35 Torr oxygen, 610 Torr helium (with 7% fluctuation from run to run) at a total flow rate of 50 ml per min.

Reaction products were analyzed by a gas chromatograph with a thermal conductivity detector. A 6 ft × $\frac{1}{8}$ in.-column of Carbosphere at 220°C was used to separate CO_2, C_2H_4, and C_2H_6, and a 15- × $\frac{1}{8}$-in. column of Carbosphere at room temperature separated O_2, CO, and CH_4.

An OMNISORP BET apparatus was used to conduct surface area measurements. Catalyst surface areas after reaction were found to be very small, ranging from 0.6 to 3.9 m^2/g, comparable to the measurement error of the BET instrument. The measured values exhibited poor reproduc-

ibility from run to run and no dependence on lithium loading. Since the measured surface areas were clearly insignificant, the possible effects of surface area on the apparent reactivity were not considered in the data analysis. In other words, it was assumed that catalysts prepared from LiOH and MgO with different lithium loadings possessed similar surface areas.

XPS measurements were performed with a VG ESCALAB/SIMSLAB. A high-pressure cell was attached to the vacuum system for sample treatment. Catalyst samples for XPS studies were pressed into 10-mm disks and mounted on a standard VG transferrable sample holder. Samples could be transferred between the high-pressure cell and the ESCA analytical chamber without exposure to atmosphere. This permitted analysis of the catalyst surface composition after treatment under various conditions. All catalyst samples were subject to charging. For samples with detectable magnesium XPS signals, core level peak positions are reported as binding energies (BE) referenced to the Mg(2*p*) level at 50.8 eV. For samples without detectable magnesium signals such as Li_2CO_3, Li_2O, LiOH, and Li/MgO catalysts encapsulated by lithium species, peaks were aligned to the Li (1*s*) level at a binding energy of 56.9 eV established by reference to the Mg(2*p*) level on Li/MgO samples where both lithium and magnesium signals were detectable.

RESULTS

As mentioned previously, Lunsford *et al.* (*16*) have measured the CH_4 conversion and the C_2 selectivity from Li/MgO catalysts with different lithium loadings. In that study, the minimum lithium loading was 0.2 wt%, and no correlation between loading and activity was observed. The current work covers a wider range of lithium loadings from 0.02 to 10 wt%. Reactions were conducted at 650°C with a $CH_4/O_2/He$ feed described above. All the catalysts exhibited an initial deactivation; therefore, kinetic data reported here were collected after the catalysts had been on stream for 200 min, by which point the activity was relatively stable. The CH_4 and O_2 conversion, C_2 selectivity, and product distribution as a function of lithium loading are summarized in Table 1 and depicted in Fig. 1. The same amount of catalyst (2 g) was used in all experiments to maintain a consistent space time. At this catalyst holding, CH_4 conversion was found to be proportional to the amount of catalyst in the reactor. It can be

TABLE 1

Catalytic Activity of Li/MgO Catalysts of Different Li Loadings[a]

Li wt%	Conversion (%)		C_2 selectivity (%)	Product pressure (Torr)				
	CH_4	O_2		CH_4	C_2H_4	C_2H_6	CO_2	CO
0	2.0	7.9	18.0	114.66	0.07	0.14	1.92	0
0.02	4.1	—	7.6	130.99	0.04	0.18	4.74	0.42
0.05	6.2	—	9.6	122.09	0.11	0.28	6.53	0.76
0.10	7.6	37.0	17.5	126.44	0.28	0.63	8.24	0.34
0.15	9.3	44.4	25.7	106.69	0.49	0.92	7.87	0.25
0.20	8.2	38.3	35.7	117.21	0.67	1.20	6.39	0.34
0.25	9.6	36.8	30.8	111.87	0.63	1.20	7.97	0.25
1.00	9.1	44.8	36.4	124.66	0.91	1.34	7.56	0.42
5.00	8.0	30.4	34.5	117.53	0.53	1.23	6.53	0.17
7.00	6.0	27.4	30.6	122.83	0.21	0.99	5.36	0.08
10.00	7.6	—	35.6	124.74	0.70	1.13	6.18	0.42

[a] Conditions: 130 Torr CH_4, 35 Torr O_2, 610 Torr He; total flow rate 50 ml/min; 650°C; 2-g catalysts.

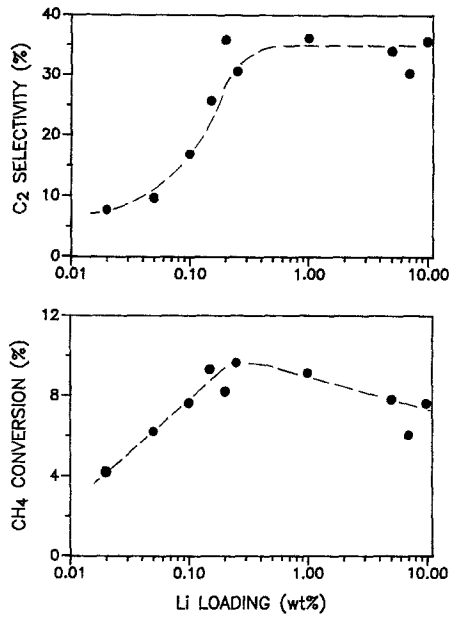

FIG. 1. CH_4 conversion and C_2 selectivity as a function of lithium loading.

seen from Fig. 1 that both CH_4 conversion and C_2 selectivity increased with lithium loading for loadings below 0.2 wt%. At higher loadings, the C_2 selectivity became roughly constant while the CH_4 conversion no longer correlated with lithium loading. The increase of CH_4 conversion with lithium loading in the low loading region certainly indicates a correlation between CH_4 activation and surface lithium concentration, although the leveling-off of this dependence at higher loading is puzzling. In an effort to resolve this problem and to understand the surface composition, catalysts with different lithium loadings were studied by XPS.

A typical XPS experiment was conducted as follows. First, a fresh Li/MgO catalyst was examined by XPS. This sample was then transferred to the VG high-pressure cell and treated under O_2 at 460°C for 2 h, simulating the O_2 calcination treatment used in kinetic experiments. After the O_2 treatment, the sample was transferred back to the analytic chamber for surface composition measurements. A third set of XPS spectra was collected from the sample after treatment in the VG high-pressure cell in the reactant stream (O_2/CH_4/He) at 650°C for 200 min. The catalysts with these three different histories are designated as *fresh, calcined,* and *used* catalysts or samples in the following discussion.

Figure 2 displays representative C(1*s*) and O(1*s*) spectra from *fresh* (a), *calcined* (b), and *used* (c) Li/MgO catalysts having a 0.2 wt% lithium loading. The *fresh* sample revealed large amorphous carbon peak at 285.8 eV and a small carbonate peak at 290.6 eV, which probably resulted from background contamination and CO_2 adsorption. The O(1*s*) spectrum from the *fresh* sample exhibited a single, symmetric peak at 531.8 eV. As will be seen in the discussion section below, this binding energy corresponds to bulk magnesium hydroxide, indicating that $Mg(OH)_2$ was the dominant phase in *fresh* Li/MgO catalysts. This fact is expected, since MgO was mixed with H_2O during sample preparation, converting MgO into $Mg(OH)_2$ (*21*).

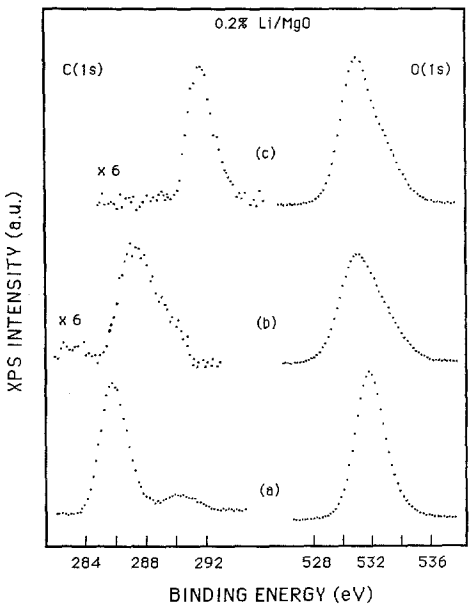

FIG. 2. C(1*s*) and O(1*s*) spectra from a 0.2 wt% Li/MgO catalyst. (a) Fresh; (b) treated by O_2 at 460°C; (c) treated by O_2/CH_4 at 650°C.

After the *fresh* catalyst was treated under O_2 at 460°C for 2 h to produce a *calcined* sample, the carbon peaks diminished drastically (Fig. 2b), indicative of carbon removal via oxidation to CO/CO_2. The small peak at 286.3 eV present after calcination may be due to residual surface carbon. The absence of any carbonate carbon, which would produce a C(1*s*) peak at higher binding energy, indicates that the surface lithium species prior to reaction was not in the form of lithium carbonate. The O(1*s*) spectrum exhibited a shift from the *fresh* catalyst to 530.7 eV upon calcination, and a new O(1s) peak appeared as a shoulder on the high-binding-energy side of the major O(1*s*) peak. This high-binding-energy peak was resolved with software provided by the instrument manufacturer and found to be centered at 533.0 eV (see Fig. 3). (In peak synthesis, the major O(1*s*) peak was fit first based on the peak maximum and the shape of the left side edge of the peak. The remainder was then fit with a second peak. At a pass energy of 5 eV, the major peak has a FWHM of 2.0 eV, while the high-binding-energy peak has a slightly larger FWHM, 2.2 eV.) The major O(1*s*) peak at 530.7 eV can be assigned to magnesium oxide according to its binding energy value (see Discussion). The shift of the O(1*s*) peak from 531.8 to 530.7 eV upon calcination therefore indicates the conversion of $Mg(OH)_2$ into MgO. The assignment of the O(1*s*) shoulder will be discussed in detail later. For clarity of the discussion below, the major O(1*s*) peak at 530.7 eV and the small O(1*s*) peak at 533.0 eV are referred as the *oxide peak* and the *O(1s) shoulder*, respectively.

Further treatment under reaction conditions brought about little change in the O(1*s*) spectrum, but produced a C(1*s*) peak at 291.6 eV (Fig. 2c). This peak can be assigned to lithium carbonate by comparison with spectra from pure Li_2CO_3. Li/MgO and Li_2CO_3 XPS spectra are compared by aligning the Li(1*s*) peaks as described under Experimental. The C(1*s*) binding energy from pure Li_2CO_3 is 291.4 eV, essentially the same as the C(1*s*) peak shown in Fig. 2c. Lithium carbonates on the *used* catalyst may be formed by reaction between surface lithium and gas-phase reaction products such as CO_2 and CO. Lithium carbonate has been detected as a stable phase on Li/MgO catalysts under the methane oxidative coupling conditions by X-ray powder diffraction (*16*).

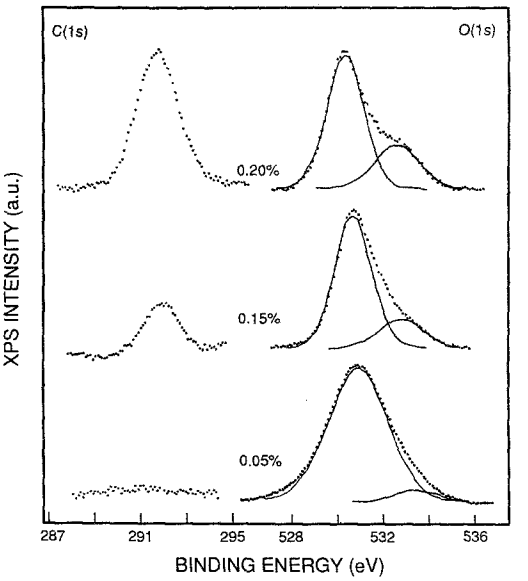

FIG. 3. C(1*s*) and O(1*s*) XPS spectra from Li/MgO samples of different Li loadings. Note that different passing energies were used while collecting these spectra: 50 eV for spectrum (a), 5 eV for spectra (b) and (c). That is why the FWHM of spectrum (a) is much greater than those of spectra (b) and (c).

Similar changes in XPS spectra with catalyst treatment were observed from Li/MgO catalysts with different lithium loadings, although the intensities of the carbonate peak and the O(1*s*) shoulder from the used catalysts depend on lithium loading. This dependence is illustrated in Fig. 3 for three representative examples. The C(1*s*) and O(1*s*) peak positions from the *calcined* and *used* samples varied slightly from sample to sample. Averaging over all the *calcined* and *used* samples yields a C(1*s*) peak from carbonate carbon at 291.6 ± 0.1 eV, an oxide O(1*s*) peak at 530.7 ± 0.1 eV,

TABLE 2

XPS Binding Energies of Selected Species (in eV)[a]

Sample	Peak position and assignment	
	C(1*s*)	O(1*s*)
Fresh MgO/H_2O	—	531.8, $Mg(OH)_2$
MgO upon calcination and reaction	—	530.7, MgO
Fresh Li/MgO	285.8, carbon deposit 290.5, adsorbed CO_2	531.8, $Mg(OH)_2$
Li/MgO after reaction	291.6, Li_2CO_3	530.7, MgO 533.0, Li^+O^- and Li_2CO_3
Li_2CO_3[b]	291.4, Li_2CO_3	532.9, Li_2CO_3
Li_2O[c]	—	531.7, Li_2O
Li_2O/H_2O[c]	—	531.7, Li_2O 534.6, LiOH

[a] Binding energies from MgO and Li/MgO samples were referenced to the Mg(2*p*) peak at 50.8 eV.

[b] Measured in this laboratory. The Li(1*s*) peak from this sample was aligned with the Li(1*s*) peak at 56.9 eV observed from Li/MgO samples.

[c] From Ref. (*22*). The peak positions were realigned with the Li(1*s*) peak at 56.9 eV observed in this study from Li/MgO samples.

and an O(1*s*) shoulder at 533.0 ± 0.3 eV. Experiments conducted with pure MgO samples revealed a similar shift of the major O(1*s*) peak from the hydroxide position (531.8 eV) to the oxide position (530.7 eV) after treatment by O_2 calcination and reaction conditions. However, neither the C(1*s*) carbonate peak nor the O(1*s*) shoulder was ever observed in the absence of lithium. This suggests that the species corresponding to the carbonate peak and the O(1*s*) shoulder on the *calcined* and *used* Li/MgO catalysts were associated only with surface lithium. The binding energies of the C(1*s*) and O(1*s*) peaks from different samples are listed in Table 2 along with their assignments.

The assignment of the O(1*s*) shoulder is of essential interest because it contains information about the surface lithium species. Three oxygen-containing lithium species are likely to be present on the *used* Li/MgO catalysts, i.e., Li_2CO_3, Li_2O, and LiOH. However, the O(1*s*) peak positions from Li_2O and LiOH reported in the literature (*22*) do not align with the O(1*s*) shoulder position, being 1.3 eV below and 1.6 eV above, respectively (see Table 2). Therefore, contributions from Li_2O and LiOH to the O(1*s*) shoulder can be excluded. If aligned by the Li(1*s*) binding energy observed from Li/MgO samples, the O(1*s*) peak from the pure Li_2CO_3 sample measured in this laboratory is at 532.9 eV, essentially the same position as the O(1*s*) shoulder (533.0 eV). In conjunction with the observation of a carbonate C(1*s*) peak from the *used* catalysts, it can be concluded that Li_2CO_3 contributes to the O(1*s*) shoulder. In addition to this argument based on binding energy positions, the predominance of Li_2CO_3 over Li_2O on MgO under the reaction conditions was also supported by another experiment. A 7 wt% Li/MgO sample treated under CO_2 at 650°C and then under reaction conditions for 200 min produced only single C(1*s*) and O(1*s*) peaks and no magnesium signals. The spectra were identical, both in the peak position and in the O(1*s*)/C(1*s*) peak area ratio, to those from the pure Li_2O_3 sample. These facts indicate that MgO in this sample was encapsulated completely by lithium carbonate, with no indication of any LiOH or

TABLE 3

XPS and Kinetic Results from Different Li/MgO Samples

Sample (wt%)	Fraction of the O(1*s*) shoulder[a] (%)	O(1*s*)[b] / C(1*s*)	CH_4 conversion (%)
0	0.9	∞	2.0
0.02	6.7	∞	4.1
0.05	7.5	∞	6.2
0.10	10.7	118.5	7.6
0.15	19.9	24.8	9.3
0.20	28.2	16.9	8.2
0.25	23.9	15.3	9.6
1.0	16.2	20.0	9.1
10.0	15.6	19.3	7.6
Li_2CO_3[c]	—	7.2	—

[a] Defined as the area of the O(1*s*) shoulder divided by the total area of the O(1*s*) peaks (the major peak plus the shoulder).

[b] The ratio of the area of the O(1*s*) shoulder (533.1 eV) to that of the C(1*s*) peak at 291.6 eV.

[c] Pure commercial sample.

Li_2O. Little change in the O(1*s*)/C(1*s*) peak area ratio was observed after further treatment under O_2, indicating that Li_2CO_3 was the stable bulk lithium phase under the reaction conditions. A similar observation has been reported by Kimble and Kolts in a thermogravemetric study (*20*).

If lithium carbonate was the only lithium species responsible for the O(1*s*) shoulder, the ratio of the areas of the O(1*s*) shoulder and the carbonate C(1*s*) peak from *used* Li/MgO catalysts should be equal to that measured from Li_2CO_3. However, the measured ratio from the *used* Li/MgO catalysts was always larger than that from the pure Li_2CO_3 sample. The extreme example of this observation was the O(1*s*) shoulder observed from *calcined* Li/MgO samples, which did not exhibit any carbonate C(1*s*) peak (Figs. 2b and 2c). This suggests that there exists another lithium species on the *calcined* and *used* catalysts besides Li_2CO_3. Li^+O^- appears to be the best candidate. This species has been detected by EPR on Li/MgO catalyst, and assigned to be the active phase on Li/MgO catalysts for methane oxidative coupling (*16*). Li^+O^- presumably can be formed by substituting lithium ions into MgO lattices (*16, 23*). Further discussion on this assignment will be given in the next section.

The relative contributions to the O(1*s*) shoulder from Li_2CO_3 and Li^+O^- can be determined as follows. The fraction from Li_2CO_3 was estimated by multiplying the area of the carbonate C(1*s*) peak at 291.6 eV by the O(1*s*)/C(1*s*) peak area ratio measured from the pure Li_2CO_3 sample. The remaining portion of the shoulder then is from Li^+O^-. The O(1*s*)/C(1*s*) ratios from different samples are listed in Table 3. With this calculation, the concentrations of surface lithium species from the *used* catalysts were monitored as a function of lithium loading. As shown in Fig. 4, the concentration of the total lithium species, defined as the area of the O(1*s*) shoulder normalized by the total area of the O(1*s*) peaks, i.e., the oxide peak plus the O(1*s*) shoulder, increased with lithium loading until 0.2 wt% followed by a sudden decrease and a relative flat region. It can also be seen that the major contribution to the O(1*s*) shoulder at the early stage (<0.1 wt%) was from surface Li^+O^- species. Above 0.1 wt%, the contribution from Li_2CO_3 became significant, and the concentrations of both surface Li_2CO_3 and Li^+O^- species increased with lithium loading until 0.2 wt%, with the concentration of Li_2CO_3 increasing faster

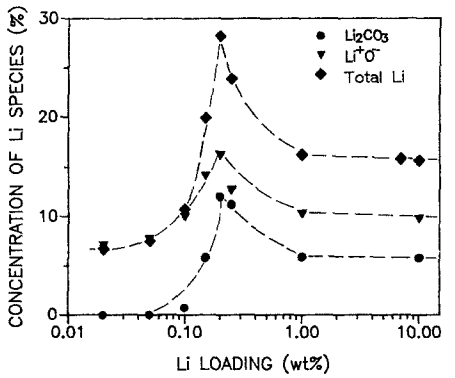

FIG. 4. Concentrations of Li_2CO_3 and Li^+O^- species as a function of lithium loading.

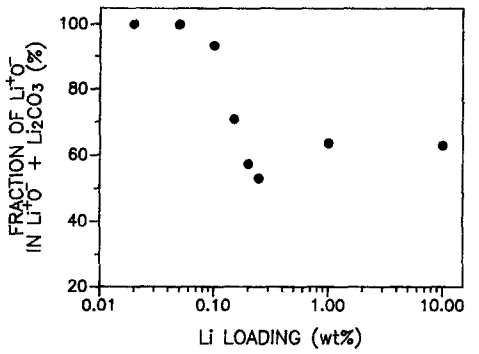

FIG. 5. Proportion of surface Li_2CO_3 and Li^+O^- species as a function of lithium loading.

than that of Li^+O^-. Above this loading, the concentrations of both species decreased, then stabilized eventually at constant levels. The change in the relative proportion of these two species with lithium loading is depicted in Fig. 5.

It was proposed above on the basis of kinetic results that there should exist a correlation between the CH_4 conversion and the concentration of surface lithium compounds. This suggestion was borne out by the XPS experiments. Figure 6 depicts the CH_4 conversion as a function of the Li^+O^- and Li_2CO_3 concentrations, defined as described above. The lithium loading of the catalysts used in this plot ranges from 0.02 to 10 wt%. It can be seen that the CH_4 conversion correlates well with the concentration of surface Li^+O^- species for all the catalysts, but not with that of Li_2CO_3. The good correlation between CH_4 conversion and the concentration of surface Li^+O^- species indicates that the surface Li^+O^- species are responsible for methane activation, in agreement with the assignment by Lunsford *et al.* (*16, 17*). The decrease and leveling-off of the concentration of these species at lithium loadings larger than 0.2 wt% explains why the correlation between the CH_4 conversion and lithium loading did not hold in this region, a question posed previously (cf. Fig. 1). Figure 6 also suggests that the surface Li_2CO_3 phase is inactive for methane activation. This assessment can be supported further by the following observation. A Li_2CO_3-encapsulated Li/MgO sample, due to heavy loading (20 wt%), did not exhibit any activity toward CH_4 conversion under the reaction conditions. The contribution from Li_2CO_3 on Li/MgO catalysts to CH_4 activation was also reported to be insignificant by Lunsford and co-workers (*16*).

DISCUSSION

In the last section, the single O(1*s*) peak at 531.8 eV from the *fresh* catalysts and the major O(1*s*) peak at 530.7 eV from the *calcined* and *used* catalysts were assigned to magnesium hydroxide and magnesium oxide, respectively. These assignments are based on the following consideration. The O(1*s*) binding energies of magnesium oxide, bulk magnesium hydroxide, and surface hydroxyl groups reported in the literature have not been very consistent, if aligned by the Mg(2*p*) level (*24–27*), most probably due to differences in instrument calibration and sample charging. Their relative positions, however, have been well established. The O(1*s*) binding energy of surface hydroxide is 2.1 to 2.4 eV higher than that of magnesium oxide (*24, 26, 27*), while bulk magnesium hydroxide exhibited a binding energy in between, i.e., 1.1 eV above the oxide peak (*25*). Two O(1*s*) peaks from the Li/MgO samples mentioned above were assigned based on this binding energy or-

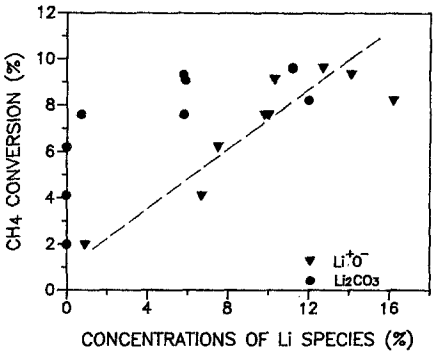

FIG. 6. CH_4 conversion as a function of the concentrations of surface Li^+O^- (▲) and Li_2CO_3 (●).

der. First, the assignment of the major O(1*s*) peak from *calcined* and *used* catalysts to magnesium oxide can be justified by its lowest O(1*s*) binding energy, 530.7 eV; furthermore, it is close to the O(1*s*) peak position from a MgO single-crystal sample measured with the same ESCA instrument, 530.4 eV. The O(1*s*) peak from the *fresh* catalyst with a binding energy 1.6 eV above the oxide peak apparently falls into the region of bulk magnesium hydroxide.

The contribution from Li^+O^- species to the O(1*s*) shoulder was assumed in the last section based on the O(1*s*)/C(1*s*) peak area ratio and the EPR measurements reported in the literature. Verification of this assignment from measured binding energy of the O(1*s*) shoulder is not straightforward. The O(1*s*) binding energy of the O^- species in Li/MgO or MgO samples has not been reported previously, and measurements on authentic samples are hampered by the instability of Li^+O^- species. Li^+O^- is reported (*16*) to be unstable under vacuum or ambient air conditions if the sample is cooled slowly after reaction, as evidenced by the absence of detectable Li^+O^- EPR signal. Since the XPS experiments reported here involved transfer of the sample from the high-pressure cell to the analytic chamber followed by set-up for XPS operation, a procedure which usually required more than 30 min, direct detection of Li^+O^- centers by XPS is improbable. However, the measured binding energy of the O(1*s*) shoulder is consistent with an argument for the indirect detection of surface Li^+O^-. In addition to the reaggregation of lithium ions in the MgO lattice which was proposed as an explanation for the disappearance of Li^+O^- signal in the EPR experiments (*23*), the Li^+O^- centers in surface layers within the XPS sampling range would be destroyed more quickly during sample transfer by another mechanism, namely, reaction with residual water vapor in the ambient vacuum. A Li^+O^- center could readily abstract a hydrogen from water, forming a surface hydroxide (denoted as Li^+OH^- according to Lunsford's nomenclature (*16*)), a process similar to that proposed by Lunsford *et al.* in the methane activation mechanism (*16, 17*). In this case, the Li^+O^- species will not be detected in its active form but in its resting form, i.e., Li^+OH^-. We believe this to be the case in our experiments. The binding energy in Li^+OH^- has never been measured, but one may expect it to be similar to that of surface OH. Indeed, the binding energy of the O(1*s*) shoulder is nearly equal to that of surface OH on MgO. The measured binding energy difference between the O(1*s*) shoulder and the oxide peak, 2.3 eV, is also consistent with binding energy differences reported for O^- and oxide oxygen in CaO and BaO, 2.6 and 2.1 eV, respectively (*26*). In the latter case a critical evaluation of the experimental procedure suggests that these materials were also in their hydroxylated resting state.

The assignment of a portion of the O(1*s*) shoulder to Li^+O^- is also supported by the variation of its intensity with lithium loading. Figure 4 demonstrates that the surface lithium is essentially in the form of Li^+O^- below 0.1 wt% loading. The formation of Li^+O^- at low lithium loadings suggests that this phase is thermodynamically preferred over Li_2CO_3, indicative of a strong interaction between lithium and the MgO lattice in the Li^+O^- centers. The onset of Li_2CO_3 formation at 0.1 wt% loading suggests that the sites for Li^+O^- formation were approaching saturation at this stage. Abraham *et al.* (*23*) have produced Li^+O^- centers in MgO single crystals by low-temperature ionizing irradiation, electron irradiation, and arc-fusion techniques using MgO powders doped with Li_2CO_3. The stable concentration of Li^+O^- in the MgO lattice prepared by the arc-fusion technique is reported to be approximately 0.03 to 0.05 at.%. If one assumes that all the MgO was involved in this lithium substitution reaction, a 0.2-wt% Li/MgO catalyst corresponds to a lithium concentration of 0.6 at.%, an order of magnitude larger than the

reported value. Given the different materials (single crystal vs amorphous MgO) and chemical environments between the current study and Abraham's, this discrepancy may not be as surprising as it appears.

Figure 4 also demonstrates that the total concentration of the surface lithium species, i.e., Li^+O^- and Li_2CO_3, increases with lithium loading until 0.2 wt%. Above this loading, the concentration decreases and remains at a constant level, although the initial loading increases from 0.2 to 10 wt%. The leveling-off of the total concentration of surface lithium species at high lithium loading may result from evaporation of the surface lithium to the gas phase and/or diffusion into the MgO bulk. The results above suggest that the catalyst surface was saturated with Li^+O^- species at a loading of around 0.2 wt%. Any additional amount of lithium above this loading thus must be present in other forms such as Li_2CO_3 and LiOH. (Note that LiOH was used as the precursor in the present work.) Due to the low melting points of these species and the weak interaction between them and the MgO support, most of these species on the catalyst surface may be volatile at the reaction temperature, leaving the surface with a saturated amount of Li^+O^- and a small amount of Li_2CO_3. In fact, contamination of the walls of the quartz reactor by lithium has been observed in this laboratory, and the loss of alkali metals to the gas phase at high temperature has been reported in the literature (*10*). However, one must note that this explanation contradicts the observation by Lunsford *et al.* (*17*) that the Li^+O^- concentration increased with lithium loading until 13.5 wt%, a loading much higher than 0.2 wt%. Barring an explanation due to the different precursors (Li_2CO_3 vs LiOH) used in two studies, this suggests another mechanism for the saturation of surface lithium concentration, namely lithium diffusion into the MgO bulk. This mechanism cannot be confirmed by the current study. The present work merely demonstrates that there is a saturation concentration of lithium species on Li/MgO catalyst surfaces. In addition to the XPS evidence, the similarity in surface composition for the catalysts with initial lithium loading above 0.2 wt% is supported by the constant C_2 selectivity from these catalysts as shown in Fig. 1. The slight scatter of the measured CH_4 conversion in this region may result from different extents of sintering for the catalysts with different initial loadings, resulting in changes in surface properties such as specific surface area. The reason for the sudden decrease of the concentration of total surface lithium species at 0.2 wt% is not clear at the present time. It may result from the segregation, phase transition, or sintering of lithium species in the surface layers at this loading.

CONCLUSIONS

Two lithium phases, i.e., Li^+O^- and Li_2CO_3, were observed on the surface of Li-doped MgO catalysts under the reaction conditions. A correlation between CH_4 conversion and the surface Li^+O^- concentration demonstrates that Li^+O^- species are the active centers for methane conversion. The surface concentration of lithium species appears to reach saturation at a lithium loading of around 0.2 wt%; the extra portion of the surface lithium from the initial loading possibly evaporated from the surface and/or diffused into the MgO bulk under the reaction conditions.

REFERENCES

1. Keller, G. E., and Bhasin, M. M., *J. Catal.* **73,** 9 (1982).
2. Hinsin, W., Bytyn, W., and Baren, M., *in* "Proceedings, 8th International Congress on Catalysis, Berlin, 1984," Vol. III, p. 581. Dechema, Frankfurt-am-Main, 1984.
3. Asami, K., Hashimoto, S., Shikada, T., Fujimoto, K., and Tominaga, H., *Chem. Lett.*, 1233 (1986).
4. Bytyn, W., and Baren, M., *Appl. Catal.* **28,** 199 (1986).
5. Moriyama, T., Takasaki, N., Iwamatsu, E., and Aika, E., *Chem. Lett.*, 1165 (1986).
6. Matsuura, I., Utsumi, Y., Nakai, M., and Doi, T., *Chem. Lett.*, 1981 (1986).
7. Otsuka, K., Liu, Q., Hatano, M., and Morikawa, A., *Chem. Lett.*, 467 (1986).

8. Otsuka, K., Jinno, K., and Morikawa, A., *Chem. Lett.*, 499 (1985).
9. Otsuka, K., Liu, Q., Hatano, M., and Morikawa, A., *Chem. Lett.*, 903 (1986).
10. Iwamatsu, E., Moriyama, T., Takasaki, N., and Aika, K., *J. Catal.* **113,** 25 (1988).
11. Sofranko, J. A., Leonard, J. J., and Jones, C. A., *J. Catal.* **103,** 302 (1987).
12. Cambell, K. D., Zhang, H., and Lunsford, J. H., *J. Phys. Chem.* **92,** 750 (1988).
13. Otsuka, K., Said, A. A., Jinno, K., and Komatsu, T., *Chem. Lett.*, 77 (1987).
14. Emesh, I. T. A., and Amenomiya, Y., *J. Phys. Chem.* **90,** 4785 (1986).
15. Lee, J. S., and Oyama, S. T., *Catal. Rev. Sci. Eng.* **30,** 249 (1988).
16. Ito, T., Wang, J.-X., Lin, C.-H., and Lunsford, J. H., *J. Amer. Chem. Soc.* **107,** 5062 (1985).
17. Driscoll, D. J., Martir, W., Wang, J.-X., and Lunsford, J. H., *J. Amer. Chem. Soc.* **107,** 58 (1985).
18. Zhang, H.-S., Wang, J.-X., Driscoll, D. J., and Lunsford, J. H., *J. Catal.* **112,** 366 (1988).
19. Lin, C.-H., Wang, J.-X., and Lunford, J. H., *J. Catal.* **111,** 302 (1988).
20. Kimble, J. B., and Kolts, J. H., *CHEMTECH* **17,** 501 (1987).
21. Cotton, F. A., and Wilkinson, G., "Advanced Inorganic Chemistry" (4th ed.). Wiley, New York, 1980.
22. Hoenigman, J. R., and Keil, R. G., *Appl. Surf. Sci.* **18,** 207 (1984).
23. Abraham, M. M., Chen, Y., Boatner, L. A., and Reynolds, R. W., *Phys. Rev. Lett.* **37,** 849 (1976).
24. Peng, X. D., Ph.D. dissertation, University of Delaware (1988).
25. Vinek, H., Latzel, J., Noller, H., and Ebel, M., *J. Chem. Soc. Faraday Trans. 1* **74,** 2092 (1978).
26. Inoue, Y., and Yasumori, I., *Bull. Chem. Soc. Japan* **54,** 1505 (1981).
27. Onishi, H., Egawa, C., Aruga, T., and Iwasawa, Y., *Surf. Sci.* **191,** 479 (1987).